

PAPER • OPEN ACCESS

Alanine response to low energy synchrotron x-ray radiation

To cite this article: P van den Elzen et al 2023 Phys. Med. Biol. 68 065011

View the article online for updates and enhancements.

You may also like

- Evaluation of alanine as a reference dosimeter for therapy level dose comparisons in megavoltage electron

Malcolm McEwen, Peter Sharpe and Sándor Vörös

- Difference in the relative response of the alanine dosimeter to megavoltage x-ray and electron beams

M Anton, R-P Kapsch, A Krauss et al.

- Response of the alanine/ESR dosimeter to radiation from an Ir-192 HDR brachytherapy source M Anton, T Hackel, K Zink et al.



Physics in Medicine & Biology





PAPER

OPEN ACCESS

RECEIVED

2 September 2022

10 January 2023

ACCEPTED FOR PUBLICATION 1 February 2023

15 March 2023

Original content from this work may be used under

the terms of the Creative Commons Attribution 4.0

Any further distribution of this work must maintain attribution to the author(s) and the title of the work, journal citation



Alanine response to low energy synchrotron x-ray radiation

P van den Elzen^{1,2,3}, T Sander¹, H Palmans^{1,4}, M McManus¹, N Woodall¹, N Lee¹, O J L Fox⁵, R M Jones^{2,3}, D Angal-Kalinin^{2,3,6} and A Subiel^{1,7}

- National Physical Laboratory, Medical Radiation Science Group, Teddington, United Kingdom
- University of Manchester, Department of Physics and Astronomy, Manchester, United Kingdom
- The Cockcroft Institute of Accelerator Science and Technology, Daresbury, United Kingdom
- MedAustron Ion Therapy Center, Wiener Neustadt, Austria
- Diamond Light Source Ltd, Harwell Science Innovation Campus, Didcot, United Kingdom
- Science and Technology Facilities Council, Accelerator Science and Technology Centre, Daresbury, United Kingdom
- University College London, UCL Cancer Institute, London, United Kingdom

E-mail: anna.subiel@npl.co.uk

Keywords: electronic brachytherapy, dosimetry, synchrotron x-rays, alanine, calorimetry, ultra-high dose rates

Abstract

Objective. The radiation response of alanine is very well characterized in the MV photon energy range where it can be used to determine the dose delivered with an accuracy better than 1%, making it suitable as a secondary standard detector in cancer radiation therapy. This is not the case in the very low energy keV x-ray range where the alanine response is affected by large uncertainties and is strongly dependent on the x-ray beam energy. This motivated the study undertaken here. Approach. Alanine pellets with a nominal thickness of 0.5 mm and diameter of 5 mm were irradiated with monoenergetic x-rays at the Diamond Light Source synchrotron, to quantify their response in the 8–20 keV range relative to 60 Co radiation. The absorbed dose to graphite was measured with a small portable graphite calorimeter, and the DOSRZnrc code in the EGSnrc Monte Carlo package was used to calculate conversion factors between the measured dose to graphite and the absorbed dose to water delivered to the alanine pellets. GafChromic EBT3 films were used to measure the beam profile for modelling in the MC simulations. Main results. The relative responses measured in this energy range were found to range from 0.616 to 0.643, with a combined relative expanded uncertainty of 3.4%-3.5% (k = 2), where the majority of the uncertainty originated from the uncertainty in the alanine readout, due to the small size of the pellets used. Significance. The measured values were in good agreement with previously published data in the overlapping region of x-ray energies, while this work extended the dataset to lower energies. By measuring the response to monoenergetic x-rays, the response to a more complex broad-spectrum x-ray source can be inferred if the spectrum is known, meaning that this work supports the establishment of alanine as a secondary standard dosimeter for low-energy x-ray sources.

1. Introduction

Dosimetry using low- and medium-energy x-ray sources remains challenging, due to the wide range of sources commercially available, and the high dose gradients inherent with photon dose depositions in this energy range (Palmer et al 2014). Current dosimetry protocols for this range of radiation qualities, included in the AAPM TG-61 and IAEA TRS-398 codes of practice (Ma et al 2001, TRS398 2001), use an in-air method for determining the dose to water from air kerma using ionisation chambers that have been traceably calibrated against primary standard free air chambers (FAC) at national measurement institutes. This method effectively determines the dose to water at the surface of a full-scatter water phantom $(D_{wz} = 0)$ for x-rays with an accelerating potential of $V \le 100$ kV. However, this approach relies on the application of backscatter factors (Klevenhagen 1982, Subiel et al 2020), which are associated with substantial uncertainties (Ma et al 2001). For medium energy x-rays with V > 100 kV, an in-phantom method is used for determining the dose to water at a depth of 20 mm. In both cases, a significant contribution of about 2% (k=1) to the uncertainty of the final measured dose to water comes from the difference in the beam quality used in calibration to that used in practice. The process also requires the conversion from air kerma to the absorbed dose to water, which requires the application of conversion and correction factors to the product of the ionisation chamber reading and the air kerma calibration coefficient of the chamber. These conversion and correction factors are defined in the codes of practice for commonly used radiation qualities (characterised by their half-value layer, or HVL) and contribute approximately another 2% (k=1) to the uncertainty. While other methods for dosimetry using quasi tissue-equivalent detectors have been used, such as diamond detectors (Yin et al 2004), films (Moradi-Kurdestany et al 2022) or Fricke solutions (O'Leary et al 2018), in this work we focus solely on alanine. Alanine has been established as a robust dosimeter in both radiotherapy and industry, including its use as a secondary standard dosimeter by several national metrology institutes (Sharpe et al 1996, Sharpe and Sephton 2000, Anton 2005, Chen et al 2008, Anton et al 2013, Khoury et al 2015, Marrale et al 2017, D'Oca et al 2019, Soliman et al 2020, Nasreddine et al 2021). However, application of alanine for very low energy x-rays (below 20 keV) has never been demonstrated. Particularly useful properties of alanine include its near tissue equivalence, wide dose range and small dose-rate dependence (Desrosiers and Puhl 2009). Its stable signal and non-destructive readout allows it to be used as a mail-in dosimeter. Therefore, there is considerable interest in extending the use of alanine as a dosimeter for low energy x-rays. The feasibility of using alanine dosimeters in this energy range is dependent on accurately quantifying the alanine response to low-energy x-rays. The alanine response has been well characterised for megavoltage (MV) photon beams and 4-25 MeV electron beams (Zeng et al 2004, Anton et al 2008) used in external beam radiation therapy (EBRT). In this range, the alanine response deviates very little from the response to the ⁶⁰Co reference beams used for calibration. Characterisation of the alanine response has made it a viable dosimeter for a range of radiation sources, including end-to-end tests in anthropomorphic phantoms (Distefano et al 2017, Carlino et al 2018) and wide-scale dosimetry audits for intensity-modulated radiotherapy (IMRT) (Budgell et al 2011).

Characterisation of the alanine response to lower energy x-rays is limited by high uncertainties and a strong energy dependence. To date, studies into the response of alanine to low energy x-rays have been carried out by Anton and Büermann (Anton and Büermann 2015), and previously by Zeng and McCaffrey (Zeng and McCaffrey 2005) and (Waldeland et al 2010) using small x-ray tubes with broad bremsstrahlung x-ray spectra, much like those used in electronic brachytherapy (eBT) and intraoperative radiotherapy (IORT). The alanine response calculated in these studies was found to be strongly dependent on the accelerating voltage of the x-ray tube. There is a limit to how well these calculated responses can be generalised to any low-energy x-ray source due to the wide range of broad-spectrum sources available, and the likelihood that a potential user of a low-energy x-ray beam will have a significantly different spectrum that yields a different alanine response. In this work, we attempt to characterise the alanine response to monoenergetic x-ray beams from a synchrotron radiation source. The use of monoenergetic beams allows for the relative response to monoenergetic x-ray beams.

2. Methodology

2.1. Radiation facility

The B16 beamline at the Diamond Light Source (DLS) synchrotron was used as a source of monochromatic x-rays in the 8–20 keV range at ultra-high dose-rates ($\sim 10~{\rm Gy~s}^{-1}$) ('B16—Diamond Light Source, Diamond 2022, Sawhney *et al* 2010). The monochromatic x-ray beams were produced by a multilayer mirror monochromator that employed a set of RuB₄C-coated mirrors for photon energies between 12 keV and 20 keV and a set of NiB₄C-coated mirrors for the 8 and 10 keV beams. The x-ray beam was monodirectional and arrived at the sample position with a divergence of 1 mrad horizontally and 0.2 mrad vertically, respectively. Adjustable slits were used to collimate the beam to a field size of approximately 6 mm \times 6 mm. A fast shutter was used to turn the beam on and off quickly and provide accurate control of the exposure time of the dosimeters positioned in the test stand. A transmission ionisation chamber with thin Kapton windows was employed to monitor the incident beam output. An x-ray camera (X-ray FDS Detector, Photonic Science), placed downstream from the experimental setup, was used to align the dosimeter setups on the sample table with the x-ray beam and to monitor the beam profile during exposures.

2.2. Portable graphite calorimeter

A small portable graphite calorimeter (SPGC), previously described by (Palmans *et al* 2004), was used as a reference detector to measure the absorbed dose to graphite from monoenergetic x-rays. A schematic diagram of the SPGC is shown in figure 1.

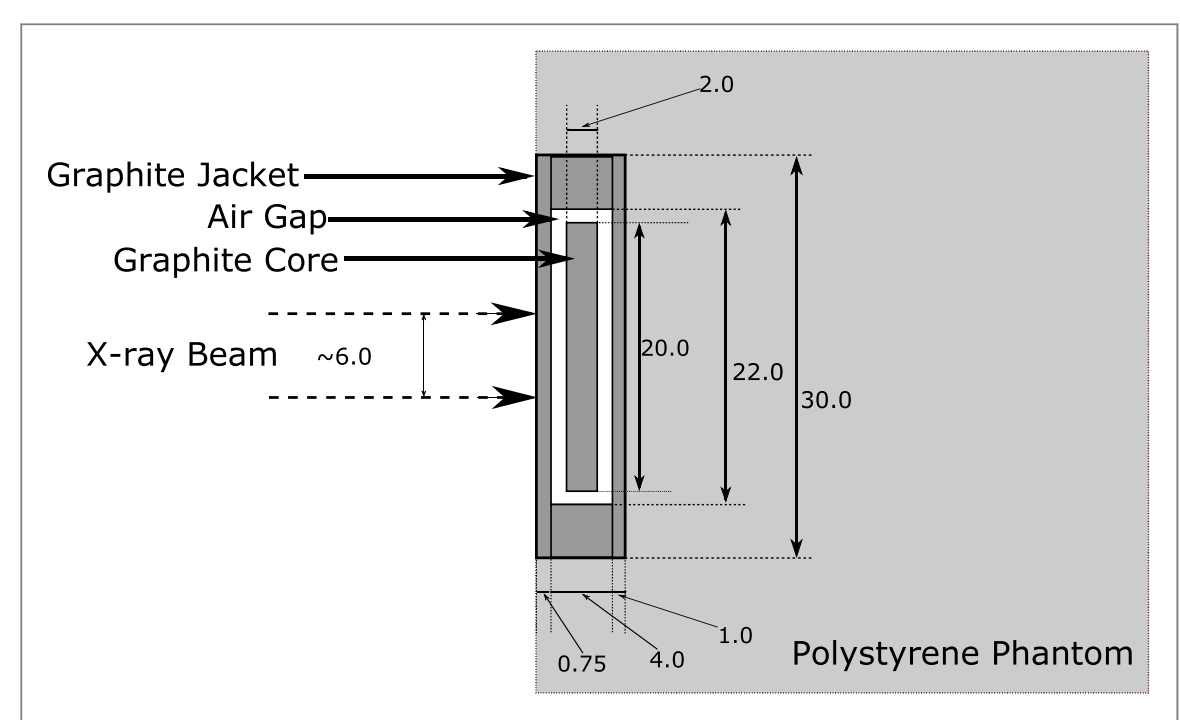


Figure 1. A cross-sectional view of the SPGC with a cylindrical geometry. The x-ray beam, arriving from the left, varied between 6.0 mm and 6.5 mm wide. For clarity, expanded polystyrene beads in the air gap are not displayed. All dimensions in the figure are approximate and given in mm.

The calorimeter had a nested construction with a cylindrical geometry and consisted of a 20 mm-diameter, 2 mm-thick core surrounded by a 30 mm-diameter, 4 mm-thick jacket with a 0.75 mm-thick front window. The SPGC core and jacket were made of Southern Graphite grade IG 11 with a grain density of 2.266 g cm $^{-3}$ and a bulk density of 1.767 g cm $^{-3}$. Thin expanded polystyrene beads were used to hold the core in place and allowed a 1 mm-wide air gap between the core and the jacket.

The SPGC incorporated seven thermistors. Four thermistors were embedded evenly around the edges of the core to measure its temperature, and two thermistors were embedded in the jacket to monitor heat flow between the core and jacket. The final thermistor was placed close to the outside of the jacket to monitor the ambient temperature. Each thermistor was connected to its own DC Wheatstone bridge and calibrated to relate the bridge out-of-balance voltage to the temperature. Controls and data acquisition were handled using in-house developed LabVIEW software and data analysis was performed using calorimetry analysis software developed at the the National Physical Laboratory (NPL).

2.3. Alanine dosimeters

Cylindrical alanine pellets, produced by Harwell Dosimeters (Harwell 2022), with a nominal diameter of 5 mm and 0.5 mm height were used. The pellets consisted of 90.9% L-alpha alanine amino acid and 9.1% paraffin wax, by weight. For the irradiations at the DLS synchrotron, the alanine pellets were placed in a phantom designed to simulate the SPGC geometry. The graphite phantom was made of HK75 isotropic graphite from Tokai Carbon with a grain density of 2.266 g cm⁻³ and a bulk density of 1.834 g cm⁻³. The alanine assembly incorporated a similar graphite jacket, however, instead of the graphite core, an alanine pellet was embedded at the centre of a graphite holder disc. The holder disc had the same diameter as the calorimeter core, but consisted of two components, a 0.77 mm-thick lid and a 1.29 mm-thick disc with a 0.54 mm-deep recess to accommodate the alanine pellet. The holder with the pellet recess is shown in figure 2. The lid and holder disc, accommodating the pellet, were placed into the graphite jacket, with poly(methyl methacrylate) (PMMA) spacers separating the core and the jacket, resembling the SPGC geometry. After each exposure, the setup was disassembled, and the alanine pellet was replaced. Each alanine pellet received at least 100 Gy to reduce the measurement uncertainty due to the low electron spin resonance signal typical for the thin pellets. For the exposures in the graphite phantom, the alanine pellets were wrapped in 0.15 mm-thick plastic film to avoid contamination from the graphite.

2.4. Radiochromic films

EBT 3 GafChromic films (GafChromic EBT-3 Dosimetry Film Specification) were used to measure the relative beam profiles. $15 \text{ mm} \times 15 \text{ mm}$ pieces of film were positioned between two graphite discs with a 20 mm diameter, which were then placed within the same graphite jacket that was used in the alanine assembly. Films

Phys. Med. Biol. **68** (2023) 065011 P van den Elzen et al

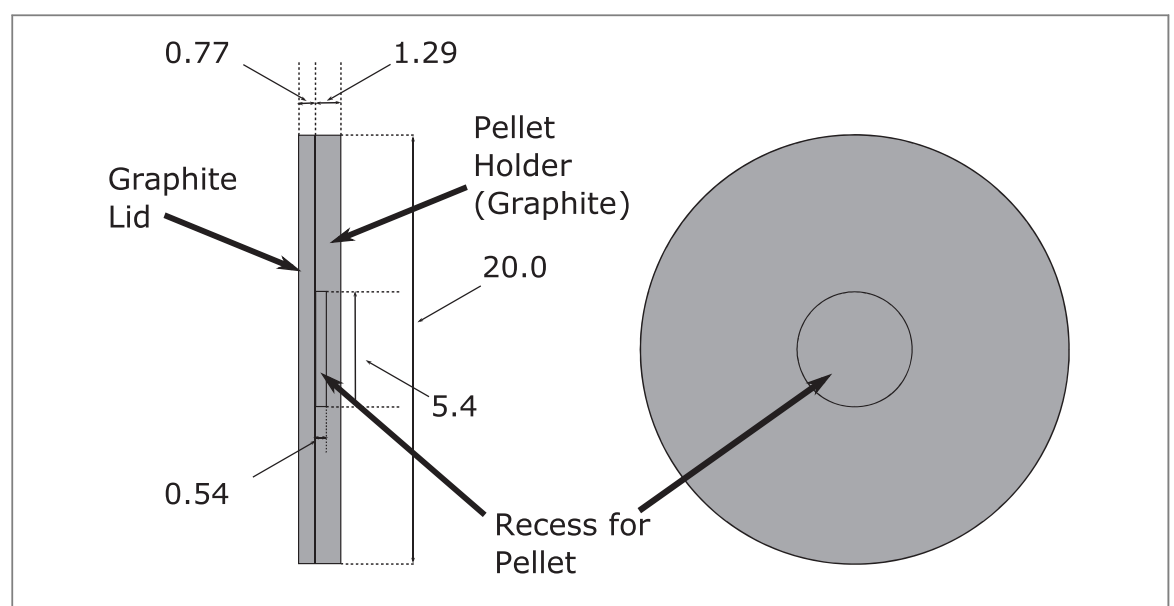


Figure 2. A cross-sectional and front view of the alanine holder plates. The surrounding jacket and polystyrene are not shown. All dimensions are approximate and given in mm.

were calibrated at the NPL using the N-20 ISO 4037 (ISO 4037-1 2019) x-ray beam with a tube potential of 20 kV in the dose range of 0–115 Gy. Six pieces of EBT 3 films (each 35 mm \times 35 mm), cut from a single sheet of film, were used to generate a calibration curve. The films were digitised with an EPSON Expression 10000XL Pro flatbed colour scanner operating in transmission mode. Coloured images were acquired with a spatial resolution of 1200 dpi, 48 bit RGB dynamic range and all colour corrections turned off. A frame was used to position the films in an area of the scanner bed which could correct optical density (OD) readings for scanner light non-uniformity (Saur and Frengen 2008). The orientation of all films was kept constant to avoid any effect due to polarised light. A 3.5 mm PMMA sheet was placed on top of the films during digitisation in order to position the films flat on the scanner bed. Any scanner warming-up effect was diminished by using 10 repeated scans. Films were scanned at least 24 h post-irradiation to allow the film optical density to stabilise (Cheung et al 2005). A region of interest of 13.5 mm \times 13.5 mm was analysed for each film in order to obtain the OD_{net} the difference between the OD before and after irradiation. The film response curve is defined as OD_{net} and the calibration film data was fitted with the function:

$$D = ab^{ODnet} + c, (1)$$

where *a*, *b* and *c* are fitting parameters.

2.5. Alanine irradiation procedure

To measure the dose from the synchrotron radiation at the DLS, the SPGC was exposed to beams with photon energies ranging from 8 to 20 keV, in 2 keV steps. The beam size was set to 6.5 mm \times 6 mm, to ensure that the alanine pellets (5 mm diameter) were fully exposed. For each beam energy, the dose output of the beam was measured by the calorimeter in terms of the dose to graphite. A calorimeter run consisted of irradiating the calorimeter 20 times. The temperature rise for each irradiation was derived by extrapolating the temperature drift curves of the core before and after the exposure to the mid-point of the irradiation interval, to compensate for any heat dissipation from the core during the irradiation interval. The mean of the temperature rises was then used to derive the dose to graphite absorbed in the core. The SPGC was then replaced with the alanine assembly. For each beam energy, between 5 and 10 alanine pellets were irradiated for the same amount of time as the calorimeter to deliver a dose in a range of 100–150 Gy. The transmission ionisation chamber placed 100 mm before the phantom surfaces was used to monitor the incident beam output for both the calorimeter and alanine setups, accounting for any deviation in the beam intensity between irradiations.

The response of alanine to a given beam quality, Q, with respect to its response to the calibration radiation, 60 Co, is given by

$$r_{O,60}_{Co} = D_{w,60}_{Co}/D_{w,O} \tag{2}$$

where $D_{w,60}$ is the dose to water derived from the electron spin resonance (ESR) signal of an exposed alanine pellet without the application of any energy-dependent correction from 60 Co to quality Q, and $D_{w,Q}$ is the calorimetrically determined dose to water delivered by the radiation with beam quality, Q. This response is the

inverse of the beam quality correction factor, k_Q , needed to obtain the dose to water for the beam quality, Q, from alanine pellets calibrated in 60 Co radiation.

2.6. Monte Carlo simulation

2.6.1. Monte Carlo codes

For conversion between the dose to graphite measured by the SPGC and the dose absorbed in the alanine in terms of the dose to water, the Monte Carlo (MC) package EGSnrc was employed (Kawrakow *et al* 2000). The necessary input data for the materials used in the experimental setups were generated using the pegs4 functionality, and water, polystyrene, air and graphite were generated with the following lower (A) and upper (U) photon (P) and electron (E) energy ranges in units of MeV: AP = 0.001, UP = 0.200, AE = 0.512, UE = 0.711. Note that for the electron energies, the rest mass of 0.511 MeV is included. Transport cutoffs for photons and electrons were both 1 keV (PCUT = 0.001 MeV and ECUT = 0.512 MeV). Photon cross-sections were generated from the XCOM cross-section library (Berger and Hubbell 1987), and NIST bremsstrahlung cross-sections were used. Parameters for Rayleigh scattering, bound Compton scattering and photoelectric absorption were switched on. The geometry was constructed using the EGSnrc user code DOSRZnrc due to the cylindrical nature of both setups. The graphite used in the SPGC and the graphite phantom for the alanine pellets had bulk densities of 1.767 g cm⁻³ and 1.834 g cm⁻³, respectively, but density-effect correction factors obtained from the NIST database ('X-Ray Mass Attenuation Coefficient,') were based on a grain density of 2.266 g cm⁻³.

To validate the MC simulations in EGSnrc, the conversion between the SPGC dose and the dose to the alanine pellets was also calculated using the Monte Carlo tool TOPAS, a front-end to Geant4 (Perl *et al* 2012). Graphite, water and polystyrene were defined based on the densities, chemical compositions and mean excitation energies, *I*, retrieved from the NIST ESTAR database (Hubbell and Seltzer 2022) (ICRU Report 1984, ICRU Report 90 2016). The *G4EmLivermorePhysics* and *G4EmStandardPhysics_option4* physics lists were used. Identical geometries and phase-space files to represent the x-ray beams were used in both the EGSnrc and TOPAS simulations and, in both cases, phase-space files were recycled so that 10⁷ histories were simulated.

2.6.2. Calculation of conversion factors

The dose to graphite measured by the SPGC, $D_{g,Q}$, was converted to the dose absorbed in the alanine pellet in terms of the dose to water, $D_{w,Q}$, with a conversion factor, $C_{w,g}$, according to

$$D_{w,Q} = C_{w,g} D_{g,Q} \text{ where } C_{w,g} = \frac{D_w^{MC}}{D_g^{MC}}$$
 (3)

and D_g^{MC} is the average dose scored in the SPGC core, equal to the total energy absorbed in the volume of the core divided by its mass. D_w^{MC} is the average dose scored in the volume of the alanine pellet substituted with water in the same beam.

For each beam energy, the radiation field was simulated using the digitised images of films exposed to the beam. Exposed films were scanned with the same conditions as those used in the calibration process. A resolution of 1200 dpi was chosen so that the edges of the beam and its complex structure could be resolved. Films were cropped to match the size of the beam aperture for each irradiation, and negligible scattering of the beam was assumed. The green channel OD_{net} of each pixel in the digitised exposed films was related to the dose to the film and therefore the fluence of photons at that point, which was assumed to be the relative intensity of the incident beam. For each exposed film, a phase-space file was written where each pixel in the film corresponded to a photon history in the file, with x- and y-coordinates corresponding to the pixel position, and a statistical weighting proportional to the beam intensity determined by the calibration factors from equation 1. The z-coordinates of the histories were chosen so that the beam would be initialised 10 mm before the phantom surfaces. The energy of each history in the phase-space files was set as the nominal beam energy. For each exposed pellet, an image was captured on the x-ray camera. On these images, the outline of the pellet was visible, therefore, for each pellet the simulated setup could be adjusted based on the position of the pellet relative to the beam axis. Modelling of the x-ray beam spectra using the x-ray Oriented Programs package, XOP 2.4 (Sánchez del Río and Dejus 2011), demonstrated that the x-ray beam from the MLM monochromator on the B16 beamline was quasi-monochromatic and included small contributions from higher order harmonics of the nominal beam energy. Around 2% of the photons in the beam were produced at these higher harmonic energies. The higher order harmonic energies were included in separate phase-space files and were included when calculating D_w^{MC} and D_g^{MC} .

Phys. Med. Biol. **68** (2023) 065011 P van den Elzen et al

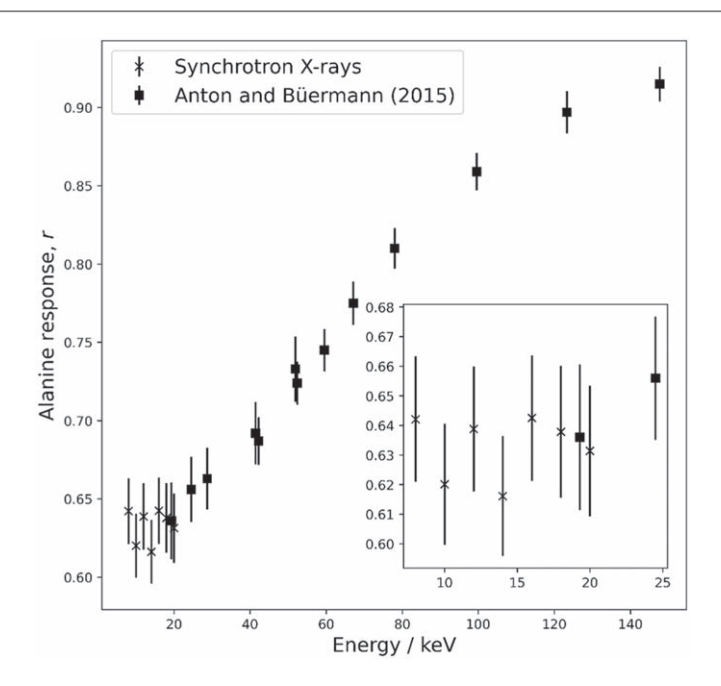


Figure 3. Plot of the response of alanine to low energy x-rays relative to 60 Co. Data from Anton & Büermann are also shown in terms of the average energy of the broad bremsstrahlung spectra used in their work with error bars taken from their paper (Anton and Büermann 2015). The inset shows the data points obtained in this work. The error bars show an uncertainty of 3.4% for the 8 keV to 16 keV points, and 3.5% for the 18 keV and 20 keV points. All error bars shown in this figure represent the expanded uncertainties (k = 2). Uncertainties in Anton & Büermann are quoted as standard uncertainties with k = 1. However, in this figure they have been converted to k = 2.

Table 1. Response factors of alanine in monoenergetic keV x-rays relative to the response to 60 Co radiation, and expanded uncertainties (k = 2).

Energy/keV	Relative response	Uncertainty / $\%$ ($k = 2$)
8	0.642	3.4
10	0.620	3.4
12	0.639	3.4
14	0.616	3.4
16	0.643	3.4
18	0.638	3.5
20	0.631	3.5

3. Results

3.1. Alanine response factors

The response factors of alanine to synchrotron x-rays in the range 8 keV to 20 keV relative to the response to 60 Co radiation, with the associated expanded uncertainties, are listed in table 1. The results are also shown in figure 3, with error bars corresponding to the uncertainties listed in table 1. Figure 3 also shows the previous results from Anton & Büermann (Anton and Büermann 2015). As the response factors they measured are for broad bremsstrahlung spectrum beams, their results are given as a function of the average energy over the spectrum. Their lowest energy x-rays were produced using an x-ray tube with a potential of $V = 30 \, \text{kV}$, and an average energy of 19.3 keV, which overlaps with the energy range explored in our work. There is an encouraging agreement between our results and those in Anton & Büermann in the region of overlapping energy. It is not possible to assign a meaningful trend to the measured alanine response factors in the 8 keV to 20 keV range. However, with the inclusion of data from Anton & Büermann it can be seen that the response curve is comparatively flat in the energy region investigated in this work.

3.2. Evaluation of uncertainties

A full breakdown of the uncertainties in the calculated response factors is given in table 2. All uncertainties in this section are quoted with a coverage factor of k = 2 (that is, a 95% confidence level), unless otherwise specified.

Table 2. A summary of the contributions to the uncertainty in the alanine response factors calculated in this work (k=2). The values in brackets apply to the data points for the 18 keV and 20 keV beams.

Uncertainty Source	Contribution (%)
Alanine Calibration	2.4
Alanine Batch Variation	1.0
Calorimeter Dose Measurement	1.1
Subtotal	2.8
Contributions due to calculation of $C_{w,g}$	
Film Calibration	0.3
Beam Centre Determination	0.6(1.2)
D_g^{MC} MC Statistics	0.2
D_w^{MC} MC Statistics	0.4
$(\mu en/\rho)_{g,w}$	1.5
Graphite Core Volume	0.1
Repeatability of Beam Profile Determination	0.7
Combined Expanded Uncertainty $(k=2)$	3.4 (3.5)

The largest contributor to the uncertainty in the calculated response factors was the alanine calibration. Uncertainty in the primary standard measured dose delivered to the alanine during calibration resulted in 2.4% uncertainty in the alanine readout. Intra-batch variation contributed a further 1.0% to the alanine readout so that the overall uncertainty associated with a single alanine pellet reading was 2.6%. The uncertainty of calorimeter measurements of the dose to graphite has a number of contributing factors. This includes a contribution of 1.0% as a type A uncertainty, obtained from 20 repeat measurements, which will also incorporate uncertainty arising due to beam instability. A contribution of 0.4% is attributed to the uncertainty in the calibration process of the thermistors (Lourenço *et al* 2022) and the uncertainty in the specific heat capacity of graphite contributes 0.2% (Williams *et al* 1993). Heat transfer correction factors were found to contribute negligible uncertainty due to the short irradiation time (Palmans *et al* 2004), and the impurity correction factors which usually arise due to the need to correct for the presence of thermistors and wires (Lourenço *et al* 2022) was not required because the thermistors and wires were not exposed to the beam. The total uncertainty in the calorimeter measurements of the dose to graphite was therefore determined to be 1.1% (k = 2), as shown in table 2. Uncertainty in the shutter opening and closing time cancels out because the calorimeter core and alanine pellets were exposed for the same amount of time.

The remaining uncertainties are associated with the calculation of the conversion factor $C_{w,g}$. The films used to determine the beam profile were calibrated using a 20 kV narrow spectrum (ISO 4037) x-ray beam where the dose was known with an estimated 4.4% uncertainty. This is a systematic uncertainty that applies to each point on the film calibration curve. A sensitivity study into the fitting parameters in equation 1 determined that this results in an uncertainty of 0.3% in the calculated values for $C_{w,v}$. The uncertainty in the determination of the centre of the beam arose from the asymmetric beam profile along the vertical axis, and poorly defined horizontal beam edges. A sensitivity study was undertaken to investigate the dependence of $C_{w,g}$ on slight changes in the y-position of the region of interest, resulting in an estimated uncertainty of 0.6% for the 8 keV to 16 keV x-ray beams, and an uncertainty of 1.2% for the 18 keV and 20 keV beams, due to the less well defined horizontal edges of the beam profiles at higher energies. The limited number of histories in the MC simulations resulted in uncertainties of 0.2% and 0.4% for D_w^{MC} and D_w^{MC} , respectively. The higher uncertainty for D_w^{MC} is due to the smaller volume of the recording region represented by the volume of the alanine pellet, compared to the volume of the graphite core used for the calculation of D_g^{MC} . The uncertainty in the graphite core volume of 0.1% results in the same uncertainty in $C_{w,g}$. A contribution to the uncertainty in $C_{w,g}$ arises from the uncertainty on mass energy-absorption ratios for low-energy photons in graphite and water, $(\mu_{en}/\rho)_{g.w}$. Based on (Andreo *et al* 2012), the uncertainty in the ratios of mass energy-absorption coefficients of graphite and water calculated using the EGSnrc 'g' user code, was found to be 1.5% for x-ray spectra with accelerating voltages of V = 25 kV to 50 kV. Finally, a set of 15 films were exposed to the 20 keV synchrotron x-ray beam. From each of these films, the same process was followed to generate a beam profile, and the conversion factor $C_{w,g}$ was calculated from each of these beams, giving a type A uncertainty of 0.7%. This uncertainty is assumed to be indicative of the repeatability of the method of simulating the synchrotron x-ray beams using films exposed to them. The combined relative expanded uncertainty (k = 2) is calculated to be 3.4% for the 8 keV to 16 keV datapoints, and 3.5% for the 18 keV and 20 keV datapoints.

4. Discussion

The dominant source of uncertainty in this work was the alanine readout, due to uncertainty in the alanine calibration factor. This value is higher in this work than in other published works due to the small volume of the alanine pellets used, so an uncertainty contribution of 2.6% (k=2) was found from the alanine readout while, for example, Anton & Büermann (Anton and Büermann 2015) found the uncertainty due to the alanine readout to be between 0.5% and 0.8%. Another significant contributor to the overall uncertainty was the determination of the delivered dose, $D_{w,Q}$. The largest contributor to this was the uncertainty in $(\mu_{enf}/\rho)_{g,w}$. This was also seen in Anton & Büermann where the main contributor to the combined uncertainty was that in the delivered dose to the alanine pellets, which was largely due to the uncertainty in $(\mu_{enf}/\rho)_{water,air}$, used in the conversion between air kerma and the dose to water.

While the combined uncertainties are comparable to those published by Anton & Büermann, they are still relatively low considering the unusual beam geometry used in this work, and lack of an established dosimetric protocol to derive $D_{w,Q}$. Specifically, the calculation of $D_{w,Q}$ was expected to be sensitive to accurate modelling of the beam, due to the difference in size of the calorimeter core and alanine pellets used in this experiment. However, as the alanine pellets were consistently fully exposed to the synchrotron x-ray beam, and the calorimeter core was consistently partially exposed, the calculated values for D_w^{MC} and D_g^{MC} were resilient to small changes in the relative beam profile and the geometry of the beam, and the overall uncertainty in $D_{w,Q}$ was instead dominated by the uncertainty in the mass energy-absorption ratio $(\mu_{en}/\rho)_{g,w}$ due to uncertainty in the photon cross sections from the XCOM database (Berger and Hubbell 1987)²⁷. While the overall uncertainty in $(\mu_{en}/\rho)_{g,w}$ is difficult to evaluate and not given explicitly by Berger & Hubbell (Andreo *et al* 2012), have established an 'envelope of uncertainty' based on a range of datasets for the mass energy-absorption coefficients of photons in various materials, and have estimated an uncertainty of 1.5% in the ratio $(\mu_{en}/\rho)_{g,w}$ for the range of x-ray energies relevant to this work. It can be reasonably assumed that a similar uncertainty will apply to a calculation of a ratio of the doses to graphite and water calculated using a MC code and photon cross sections from Berger & Hubbell.

5. Conclusions

To support the use of alanine as a secondary standard dosimeter for low-energy x-ray sources used in eBT and IORT, the response to monoenergetic synchrotron radiation with photon energies from 8 to 20 keV relative to the response to ⁶⁰Co radiation has been measured. The IPEMB kV x-rays code of practice (Klevenhagen *et al* 1996) recommends that the absorbed dose to water at the surface of a full-scatter water-equivalent phantom $(D_{w,z=0})$ can be determined from the reading of a thin-window parallel-plate ionization chamber. Based on this protocol, the relative expanded uncertainty for reference dosimetry in the very low energy x-ray beams is 6.7% (k=2) (Klevenhagen et al 1996, Ma et al 2001). In this study, alanine pellets with a nominal thickness of 0.5 mm and diameter of 5 mm have been exposed to monoenergetic x-rays at the Diamond Light Source synchrotron using a small portable graphite calorimeter as a reference dosimeter. Due to the small size of the alanine pellets used, the uncertainty on the measured response was dominated by the uncertainty in the alanine readout. This could be reduced by delivering a higher dose level to the thin alanine pellets. However, a significant uncertainty contribution in the delivered dose was also due to the use of non-standard exposure conditions and the need for MC simulations to calculate the dose delivered to the alanine pellets in terms of the dose to water, leading to a combined expanded uncertainty of 3.4%-3.5% (k=2). Regardless of the limitations of the experimental method employed in this work, this is still a factor of two lower than the uncertainty on reference dosimetry obtained with thin-window parallel-plate ionization chambers. Considering future work leading to further reduction of the measurement uncertainties, the application of a larger and uniform radiation field fully encompassing core of the calorimeter could lead to a decrease of the associated uncertainty in the determination of the $C_{g,w}$ factor.

Agreement with previous published data is found in regions of overlapping energy, and this work extends the data on the alanine response to lower-energy x-rays. Previously published data on the alanine relative response calculated with MC methods has not demonstrated satisfactory agreement with the experimental results (Zeng and McCaffrey 2005, Waldeland *et al* 2010, Anton and Büermann 2015). This has been attributed to the fact that the effect detected in ESR dosimetry is the concentration of free radicals which cannot be simulated with current models available in MC calculations. The number of radicals generated per unit absorbed dose is approximately constant for 60 Co radiation, megavoltage x-rays and electrons. However, for lower photon energies (such as those used in our study), the number of radicals per unit absorbed dose decreases. This effect can be described by an intrinsic efficiency, η , which is also called the relative effectiveness. In order to retrieve the alanine relative response based on MC calculations, the obtained result should be multiplied by the intrinsic efficiency for the

given beam energy. The intrinsic sensitivity is considered to be unity for the 60 Co reference radiation. However, the sensitivity value decreases with decreasing beam energy. This effect has also been observed in ion beams with increasing linear energy transfer (LET) (Hansen and Olsen 1985). The lowest data point for η is available for the 42.4 keV x-ray beam (Anton and Büermann 2015), which is still higher than the beam energy range used in this work. Future investigations of the intrinsic efficiency of the alanine dosimeter would be highly desirable to make theoretical predictions of response data accessible.

Also, further work is required to extend these data for monoenergetic beams, that can serve as kernel data, across the entire range of low-energy x-rays available. Characterisation of the relative response of alanine to low-energy x-rays supports its use as a dosimeter in future radiobiological and pre-clinical studies using x-rays. In particular, the dose-rate independence of alanine dosimeters means there is potential use of alanine dosimetry in studies investigating the FLASH effect (Favaudon *et al* 2014) in low-energy x-rays, where the tissue sparing properties of high dose-rate radiation may be exploited to deliver more effective and safer eBT or IORT. More recently, alanine has also been demonstrated to be a suitable detector for dosimetry of ultra-high-pulse-dose-rate electron beams (Bourgouin *et al* 2022). Further characterisation with higher energy monoenergetic x-rays would allow for the response of alanine to general broad-spectrum x-ray sources to be determined if the spectrum is well known, because the response to the components of the spectrum would be known. Extension to higher energies would not require the use of very thin pellets due to shallower dose gradients, which is likely to result in reduced uncertainties.

Acknowledgments

The projects 18NRM02 PRISM-eBT and 18HLT04 UHDpulse have received funding from the EMPIR programme co-financed by the Participating States and from the European Union's Horizon 2020 research and innovation programme. This work was also supported by UK Research and Innovation (UKRI), Science and Technology Facilities Council (STFC), Cockcroft Institute [grant number ST/V001612/1] and the University of Manchester. We acknowledge the Diamond Light Source for access to the B16 test beamline under proposal MM23439-1.

ORCID iDs

H Palmans https://orcid.org/0000-0002-0235-5118 O J L Fox https://orcid.org/0000-0001-5224-7062 A Subiel https://orcid.org/0000-0002-3467-4631

References

Andreo P, Burns D T and Salvat F 2012 On the uncertainties of photon mass energy-absorption coefficients and their ratios for radiation dosimetry *Phys. Med. Biol.* **57** 2117–36

Anton M 2005 Development of a secondary standard for the absorbed dose to water based on the alanine EPR dosimetry system *Appl. Radiat. Isot.* 62 779–95

Anton M and Büermann L 2015 Relative response of the alanine dosimeter to medium energy x-rays *Phys. Med. Biol.* **60** 6113–29 Anton M, Kapsch R P, Krauss A, von Voigts-Rhetz P, Zink K and McEwen M 2013 Difference in the relative response of the alanine dosimeter to megavoltage x-ray and electron beams *Phys. Med. Biol.* **58** 3259–82

Anton M, Kapsch R P, Krystek M and Renner F 2008 Response of the alanine/ESR dosimetry system to MV x-rays relative to (60)Co radiation *Phys. Med. Biol.* 53 2753–70

Diamond 2022 B16: Test beamline (https://www.diamond.ac.uk/Science/Research/Optics/B16)

Berger M J and Hubbell J H 1987 XCOM: Photon cross sections on a personal computer. (United States: National Bureau of Standards, Gaithersburg, MD 20899) (https://doi.org/10.2172/6016002)

Bourgouin A, Hackel T, Marinelli M, Kranzer R, Schüller A and Kapsch R-P 2022 Absorbed-dose-to-water measurement using alanine in ultra-high-pulse-dose-rate electron beams *Phys. Med. Biol.* 67 205011

Budgell G, Berresford J, Trainer M, Bradshaw E, Sharpe P and Williams P 2011 A national dosimetric audit of IMRT *Radiother. Oncol.* 99 246–52

Carlino A, Gouldstone C, Kragl G, Traneus E, Marrale M, Vatnitsky S and Palmans H 2018 End-to-end tests using alanine dosimetry in scanned proton beams *Phys. Med. Biol.* 63 055001

Chen F, Nicolucci P and Baffa O 2008 Enhanced sensitivity of alanine dosimeters to low-energy x-rays: preliminary results *Radiat. Meas.* 43 467–70

Cheung T, Butson M J and Yu P K 2005 Post-irradiation colouration of Gafchromic EBT radiochromic film *Phys. Med. Biol.* 50 N281–5 Desrosiers M F and Puhl J M 2009 Absorbed-dose/dose-rate dependence studies for the alanine-EPR dosimetry system *Radiat. Phys. Chem.* 78 461–3

Distefano G, Lee J, Jafari S, Gouldstone C, Baker C, Mayles H and Clark C H 2017 A national dosimetry audit for stereotactic ablative radiotherapy in lung *Radiother. Oncol.* 122 406–10

D'Oca M C, Marrale M, Abbene L, Bartolotta A, Collura G, d'Errico F and Principato F 2019 Alanine films for EPR dosimetry of low-energy (1–30 keV) x-ray photons *Nucl. Instrum. Methods Phys. Res.*, Sect. B 459 1–6

Favaudon V, Caplier L, Monceau V, Pouzoulet F, Sayarath M, Fouillade C and Vozenin M C 2014 Ultrahigh dose-rate FLASH irradiation increases the differential response between normal and tumor tissue in mice Sci. Transl. Med. 6 245ra293

GafChromic EBTâ3 Dosimetry Film Specification Retrieved from (http://gafchromic.com/documents/EBT3_Specifications.pdf) accessed January 2022

Hansen J W and Olsen K J 1985 Theoretical and experimental radiation effectiveness of the free radical dosimeter alanine to irradiation with heavy charged particles *Radiat*. *Res.* 104 15–27

Harwell 2022 B16: Test beamline (https://harwell-dosimeters.co.uk/harwell-alanine/) Harwell Alanine

1984 Stopping Powers for Electrons and Positrons. (MD, USA: Bethesda) ICRU Report 37

ICRU Report 90 2016 *Key data for ionizing-radiation dosimetry: Measurement standards and applications.* (Oxford: Oxford University Press) ISO 4037-1 2019 Retrieved from (https://iso.org/standard/66872.html)

Kawrakow I, Rogers D, Mainegra-Hing E, Tessier F, Townson R and Walters B 2000 EGSnrc toolkit for Monte Carlo simulation of ionizing radiation transport [release v2021]. (https://doi.org/doi:10.4224/40001303)

Khoury H J, da Silva E J, Mehta K, de Barros V S, Asfora V K, Guzzo P L and Parker A G 2015 Alanine-EPR as a transfer standard dosimetry system for low energy X radiation *Radiat*. *Phys. Chem.* 116 147–50

Klevenhagen S C 1982 The build-up of backscatter in the energy range 1 mm Al to 8 mm Al HVT (radiotherapy beams) *Phys. Med. Biol.* 27 1035

Klevenhagen S C, Aukett R J, Harrison R M, Moretti C, Nahum A E and Rosser K E 1996 The IPEMB code of practice for the determination of absorbed dose for x-rays below 300 kV generating potential (0.035 mm Al - 4 mm Cu HVL; 10 - 300 kV generating potential) *Phys. Med. Biol.* 41 2605

Lourenço A, Lee N, Shipley D, Romano F, Kacperek A, Duane S, Cashmore M, Bass G, Palmans H and Thomas R 2022 Application of aportable primary standard level graphite calorimeter for absolute dosimetry ina clinical low-energy passively scattered proton beam *Phys. Med. Biol.* 67 225021

Ma C M, Coffey C W, DeWerd L A, Liu C, Nath R, Seltzer S M and Seuntjens J P 2001 AAPM protocol for 40-300 kV x-ray beam dosimetry in radiotherapy and radiobiology *Med. Phys.* 28 868–93

Marrale M, Abbene L, d'Errico F, Gallo S, Longo A, Panzeca S and Principato F 2017 Characterization of the ESR response of alanine dosimeters to low-energy Cu-target X-tube photons *Radiat. Meas.* 106 200–4

Moradi-Kurdestany J, Bartkoski D A, Tailor R, Mirkovic D, Harel Z, Bar-David A and Salehpour M 2022 Dosimetry of a novel focused monoenergetic beam for radiotherapy *Phys. Med. Biol.* 67 07NT01 1–9

Nasreddine A, Kuntz F and El Bitar Z 2021 Absorbed dose to water determination for kilo-voltage X-rays using alanine/EPR dosimetry systems *Radiat. Phys. Chem.* **180** 108938

O'Leary M, Boscolo D, Breslin N, Brown J M C, Dolbnya I P, Emerson C and Currell F J 2018 Observation of dose-rate dependence in a Fricke dosimeter irradiated at low dose rates with monoenergetic x-rays Sci. Rep. 8 4735

Palmans H, Thomas R, Simon M, Duane S, Kacperek A, DuSautoy A and Verhaegen F 2004 A small-body portable graphite calorimeter for dosimetry in low-energy clinical proton beams *Phys. Med. Biol.* 49 3737–49

Palmer A L, Bradley D A and Nisbet A 2014 Dosimetric audit in brachytherapy Br. J. Radiol. 87 20140105

Perl J, Shin J, Schumann J, Faddegon B and Paganetti H 2012 TOPAS: an innovative proton Monte Carlo platform for research and clinical applications Med. Phys. 39 6818–37

Sánchez del Río M and Dejus R 2011 XOP v2.4: recent developments of the x-ray optics software toolkit Proc. SPIE 8141 1-5

Saur S and Frengen J 2008 GafChromic EBT film dosimetry with flatbed CCD scanner: a novel background correction method and full dose uncertainty analysis *Med. Phys.* 35 3094–101

Sawhney K J S, Dolbnya I P, Tiwari M K, Alianelli L, Scott S M, Preece G M and Walton R D 2010 A test beamline on Diamond Light Source AIP Conf. Proc. 1234 387–90

 $Sharpe\ P\ and\ Sephton\ J\ 2000\ An\ automated\ system\ for\ the\ measurement\ of\ alanine/EPR\ dosimeters\ Appl.\ Radiat.\ Isot.\ 52\ 1185-8$ $Sharpe\ P\ H,\ Rajendran\ K\ and\ Sephton\ J\ P\ 1996\ Progress\ towards\ an\ alanine/ESR\ therapy\ level\ reference\ dosimetry\ service\ at\ NPL\ Appl.$

Soliman Y S, Pellicioli P, Beshir W B, Abdel-Fattah A A, Fahim R A, Krisch M and Bräuer-Krisch E 2020 A comparative dosimetry study of an alanine dosimeter with a PTW PinPoint chamber at ultra-high dose rates of synchrotron radiation *Physica Med.* 71 161–7

Subiel A, Silvestre Patallo I, Palmans H, Barry M, Tulk A, Soultanidis G and Schettino G 2020 The influence of lack of reference conditions on dosimetry in pre-clinical radiotherapy with medium energy x-ray beams *Phys. Med. Biol.* 65 085016

TRS398 2001 Absorbed dose determination in external beam radiotherapy. (Vienna: IAEA)

Waldeland E, Hole E O, Sagstuen E and Malinen E 2010 The energy dependence of lithium formate and alanine EPR dosimeters for medium energy x rays *Med. Phys.* 37 3569–75

Williams A, Burns D and McEwen M 1993 Measurement of the specific heat capacity of the electron-beam graphite calorimeter (Vol. 94) Hubbell J H and Seltzer S M 2022 NIST Standard Reference Database 126

Yin Z, Hugtenburg R P, Green S and Beddoe A H 2004 Dose responses of diamond detectors to monoenergetic x-rays *Nucl. Instrum. Methods Phys. Res., Sect. B* 213 646–9

Zeng G G and McCaffrey J P 2005 The response of alanine to a 150keV x-ray beam Radiat. Phys. Chem. 72 537–40

Zeng G G, McEwen M R, Rogers D W and Klassen N V 2004 An experimental and Monte Carlo investigation of the energy dependence of alanine/EPR dosimetry: I. Clinical x-ray beams *Phys. Med. Biol.* 49 257–70